Mathematical Geology, Vol. 3, No. 3, 1971

The Dynamics of Shale Compaction and Evolution of Pore-Fluid Pressures[1]

J. E. Smith[2]

A mathematical model of sedimentation and compaction of fine-grained rocks such as shale has been constructed. Water is considered to flow upward or downward out of a compacting rock according to Darcy's law until the pore-water pressure within the rock is normal for the depth in question. The porosity decreases during compaction until a minimum porosity, determined by the difference between total vertical stress (overburden pressure) and pore-water pressure, is obtained. The model takes into account the dependence of permeability on porosity for a given rock type, and the dependence of water viscosity on salinity, temperature, and pressure. The derived equations have been computer programmed to obtain the time dependence of porosity, pressure, water velocity, permeability, and other factors within a compacting shale during (a) shale sedimentation, (b) a time lapse following shale deposition, (c) the deposition of normally pressured sediments over the shale, and (d) a second time lapse following deposition of the normally pressured unit. Solutions to these problems are given for the situation when the unit underlying the shale is normally pressured, and for the situation when the underlying unit is impermeable. The calculations show that a portion of a thick shale adjacent to a normally pressured unit may have a considerably reduced porosity and permeability, and act as a seal for the remainder of the shale. High fluid pressures may persist for many millions of years in thick shales with low permeability. The computations can be extended to cover more complicated cases of interbedded shales, sands, and other lithologies.
KEY WORDS: simulation, hydrology, petroleum, sedimentology, high fluid pressures, compaction, primary migration.

INTRODUCTION

Shales and other fine-grained compressible rocks are considered to be the source rocks for much petroleum found accumulated in sandstones and carbonates. Determination of the mechanism and timing of oil and gas migration out of such fine-grained rocks is a major problem. Water is the predominant fluid in these rocks, and an adequate theory of water loss by compaction, giving water velocity and pressure profiles through source rocks, would provide the basis for discussing many of the mechanisms of petroleum migration which have been proposed. These include petroleum movement in water solution or as micelles, or petroleum movement as a separate phase occupying a minor fraction of the total pore space. The primary objective of this study is to derive an adequate theory of water loss from compressible rocks during compaction, as a basis for further studies of petroleum migration.

A secondary objective is to contribute to the understanding of how higher-than-normal fluid pressures come about and what factors cause these abnormal pressures

[1] Manuscript received 26 October 1970.
[2] Phillips Petroleum Company (USA).

to persist for many millions of years. These high pressures affect seismic interpretations, casing and mud programs during drilling, and drilling safety.

The results derived in this report can be applied to any compressible fine-grained rock, so that mudstone, limy shale, or limestone may be substituted for shale in the text.

Shales commonly have porosities of 50–90 percent when deposited in sedimentary basins and lose large volumes of water when buried. In areas where the sand–shale ratio is high (>35 percent), and especially at depths less than 1000 m, the shale porosities tend to decrease steadily with depth and the pore-water pressure of adjacent and enclosed sands corresponds to that in a column of water reaching from the water table to the depth in question. These porosities and pressures are described as "normal." Thick shales may be encountered in which the porosity trend reverses, and the porosities may be greater than those found in shales at shallower depths. Sand lenses enclosed in these thicker shales may have pore-fluid pressures greater than normal, and may approach the total vertical stress or overburden pressure exerted by the overlying column of rock and water. It is generally inferred that the pore-water pressure in the enclosing shale also is greater than normal, and that the maintenance of the high pressure for long periods of time is primarily the result of the low permeability of shales.

A number of mechanisms for the creation and maintenance of high fluid pressures and high porosities in shales have been suggested.

1. Dickinson (1953) considered that high pressures are encountered in situations where the expulsion of water from shales has not been rapid enough to allow the rock framework to take up the continuously increasing weight of added sediments.

2. Harkins and Baugher (1969) state that "to develop abnormal pressures the shales usually must be over 200 feet thick," and, with some reservations, "abnormal pressure is not usually found in zones with greater than 35 percent sand." These observations and their discussion of high pressures in sands sealed against high-pressured shales along growth faults suggest that the low permeability of shales is responsible for high pressures.

3. Boatman (1967) indicated that a higher density, limy shale cap often overlies high-pressured, low-density shales. Boatman also stated that in his opinion shales "are more dense when close to sand bodies because more water has been squeezed out into the sand bodies." Both effects, presumably, could act to seal off a shale to further loss of pore-fluids. The above authors were studying the U.S. Gulf Coast.

4. Finch (1969) attributes abnormal pressures in the Antelope and Elkhorn Ranch fields in the Williston Basin to local tectonic forces accompanying structural growth.

5. Hanshaw (1962) states that "osmotic transfer of water across shales may be the cause of widespread high or low piezometric surfaces." For instance, high pressures should develop in saline waters separated from fresher, normally pressured waters by a shale unit, provided that the shale unit is permeable to water but not to salt.

6. Powers (1967) and Burst (1969) suggest that much water in montmorillonite and other clays is bound to the clays, and that its release is related to depth of burial

and probably temperature. Powers states that this release of water explains abnormal fluid pressures.

7. Heard and Rubey (1966) suggest that gypsum may release water in transforming to anhydrite, in a certain temperature–pressure range, and that the water pressure may become higher than normal.

8. Chaney (1950) considers that anomalously high pore-fluid pressures are formed as a result of the conversion of high-mol.-wt organic compounds to smaller molecules which would occupy a greater volume at the same pressure, or exert a greater pressure at the same volume.

There are some arguments favoring all the above mechanisms as contributing to the creation and maintenance of high pressures. Tkhostov (1963) discusses the conflicting opinions and tabulates for many fields pressures which are both greater and less than normal.

This investigation is based on the view that the rate of shale compaction is limited by its low permeability, and that the permeability can decrease as the porosity is reduced. In areas of rapid deposition, the loss of water from shales is thought to lag behind what is potentially possible for the existing weight of accumulated overburden. In this situation, the pore water begins to carry part of the load that would be held by the grain-to-grain contacts of the solid matrix, and the pore-water pressure becomes greater than the normal pressure. This effect will increase in magnitude for thicker shale units. If deposition ceases, water will continue to be expelled from the shale unit at a diminishing rate until the fluid pressure is reduced to normal. Renewed deposition will cause a further rise in excess pressure and the expulsion of more water. The boundary conditions adapted in the mathematical model exclude the possibility of faulting, although faults do occur in areas of high pressures and may change fluid flow rates and patterns near the faults. The possible release of some bound water within the shale is not considered, nor are the possible solution and deposition of minerals or the breaking of grains explicitly considered. For the model, the fluid in the shales is water with dissolved salts and organic materials; situations in which more than one fluid phase exists have not been considered as yet. Osmotic phenomena and conditions leading to changes in composition of the water in the shales are not considered. The intention is to deal with the mechanical problem of compacting shales by squeezing water out of them. The assumptions of the present model of high pressures are similar to the assumptions used by Rubey and Hubbert (1959) in their explanation of over-thrust faulting.

MATHEMATICAL DEVELOPMENT

The depositional environment visualized is a level surface, thousands or tens of thousands of square miles in area. Water depth is constant over the entire area, and may vary during succeeding epochs. Beginning at time zero, shale is deposited at a uniform constant rate, e.g., 0.1 m/1000 yr, over the entire area. The physical characteristics of the freshly deposited shale (mud), such as grain-size distribution, lithology, porosity, and packing geometry, are constant throughout the entire area and through-

out the depositional history. As the unit thickens there is a tendency for pore volumes to be reduced and simultaneously for water to be lost from the more deeply buried shale. Vertical and horizontal permeabilities are assumed to be of the same order of magnitude, so that water expelled must either go upward to the surface or downward to the unit below, except near the edges of the depositional area. Furthermore, the depositional environment is such that the shale does not extrude laterally and is not subjected to lateral compression. Hence the shale matrix material (grains) also is confined to downward or upward motion. These idealizations narrow the problem to considering vertical movements of the matrix and water within a vertical cylinder of unit cross section.

Figure 1 illustrates the spatial relationships and the coordinate system. The position of a differential element of pore water or solid matrix material is measured as the vertical distance Z upward (positive) from the base of the shale. The differential elements have velocities which are positive if the material in question is moving upward and negative if the material is moving downwards relative to the base of the shale. Thus, the pore water contained in the unit cross section between Z and $Z+dZ$ will have an average velocity v_w which is a function of Z, the time t, and the depositional history and boundary conditions:

$$v_w = v_w(Z, t) \tag{1}$$

Similarly, the matrix material between Z and $Z+dZ$ will have an average velocity v_r, where

$$v_r = v_r(Z, t) \tag{2}$$

The continuity equation for pore water incorporates the law of conservation of mass for the volume increment between Z and $Z + dZ$ in differential form:

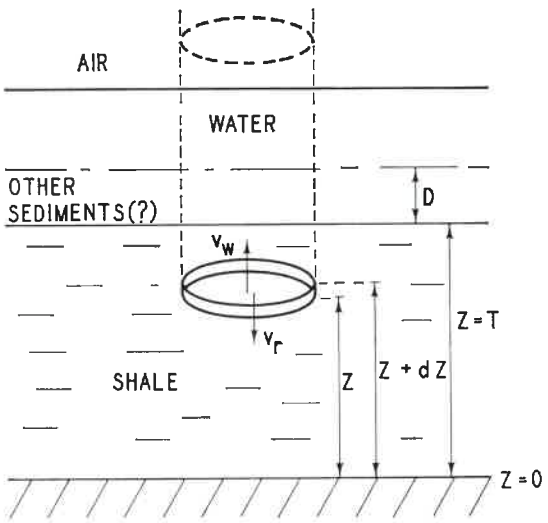

Figure 1. Shale deposition.

$$[\text{mass in at } Z \text{ during } dt] - [\text{mass out at } (Z+dZ) \text{ during } dt] = [\text{increase in mass within volume element during } dt] \tag{3}$$

The differential time increment is denoted by dt. If ϕ is the porosity and ρ_w is the density of water, these individual word descriptions become

$$\text{mass in at Z during } dt = (\rho_w v_w \phi)_Z \, dt \tag{4}$$

$$\text{mass out at } (Z+dZ) \text{ during } dt = (\rho_w v_w \phi)_{Z+dZ} \, dt \tag{5}$$

$$\text{increase in mass within volume element during } dt = (\partial \rho_w \phi / \partial t) \, dZ dt \tag{6}$$

The subscripts Z and $Z+dZ$ in eq (4) and (5) indicate the point at which the variables in parentheses are to be evaluated. Substituting back into eq (3) and dividing through by $-dZdt$ gives

$$\frac{(\rho_w v_w \phi)_{Z+dZ} - (\rho_w v_w \phi)_Z}{dZ} = \frac{-\partial \rho_w \phi}{\partial t} \tag{7}$$

or

$$\frac{\partial \rho_w v_w \phi}{\partial Z} = \frac{-\partial \rho_w \phi}{\partial t} \tag{8}$$

The continuity equation for the solid matrix material is determined by a parallel argument:

$$\frac{\partial \rho_r v_r (1-\phi)}{\partial Z} = \frac{-\partial \rho_r (1-\phi)}{\partial t} \tag{9}$$

ρ_r is the density of the solid grains.

For unit area, the instantaneous volume flow rate of water at Z relative to the solid matrix at Z is given by

$$(v_w - v_r) \phi \tag{10}$$

This quantity will be positive if water moves upward relative to the matrix material. This volume rate of flow is proportional to the negative space gradient of Ψ, the fluid potential, and inversely proportional to the viscosity of water μ:

$$(v_w - v_r) \phi = \frac{-K}{\mu} \frac{\partial \Psi}{\partial Z} \tag{11}$$

The proportionality constant K is called the permeability. Equation (11) is Darcy's law. It is the phenomenological relationship for flow in rocks including shales (Gondouin and Scala, 1958) and its use here is not intended to distinguish between laminar flow and diffusional flow. The potential gradient is given by

$$\frac{\partial \Psi}{\partial Z} = \frac{\partial \left(p - g \int_{Z=Z}^{T} \rho_w dZ - p_e \right)}{\partial Z} \tag{12}$$

where p is the local water pressure at Z, g is the gravitational constant, T is the value of the Z coordinate at the top of the sedimentary column, and p_e is the hydrostatic pressure at $Z = T$.

The three types of pressures which act in the vertical direction at Z may be discussed with reference to Figure 1. Consider that a small cylinder with rigid sides and bottom and a slightly elastic top is implanted momentarily at Z after removal of a volume of water-saturated rock of equal volume and shape. The cylinder is filled with a fluid and there is a means of measuring the fluid pressure, changing the pressure, and measuring the deflection of the top which is of unit area. The internal pressure which suffices to prevent deflection of the top supports the weight per unit area of all the overlying sediments plus the water column and air column, and is called the total vertical stress S. If ρ is the bulk density of the water-saturated rock and p_e is the fluid pressure at the top of the sedimentary column, then

$$S = g \int_{Z=Z}^{T} \rho \, dZ + p_e \tag{13}$$

The bulk density can be written in terms of porosity and the densities of solid matrix material and water:

$$\rho = \rho_w \phi + \rho_r (1 - \phi) \tag{14}$$

Substitution into eq (13) gives a more detailed representation of the total vertical stress S, where

$$S = g \int_{Z=Z}^{T} \rho_w \phi \, dZ + g \int_{Z=Z}^{T} \rho_r (1 - \phi) \, dZ + p_e \tag{15}$$

If the fluid pressure in the cylinder is reduced to the pressure of the pore water at Z, there will be no tendency for fluids to move into or out of the cylinder if a small hole is punctured in the side. The internal pressure is then the pore-fluid pressure p. The slightly elastic top will deflect at this reduced internal pressure because the overlying sediments are not perfectly rigid. In the limit that the elasticity of the top is vanishingly small, the deflection will measure the rock-frame pressure σ, which is the difference between the total vertical stress S, and the pore water pressure p:

$$\sigma = S - p \tag{16}$$

This equality is illustrated by the mechanical model of Figure 2. In each compartment or cell of this model the spring pressure σ and the water pressure p together support the cell piston and the overlying compartments and water which exert a downward total vertical stress S.

The rock-frame pressure σ acts to compress the rock frame, and tends to reduce the porosity.

It is assumed that throughout the history of sedimentation and compaction of shales the porosity is a function of the frame pressure only:

$$\phi = \phi(\sigma) \tag{17}$$

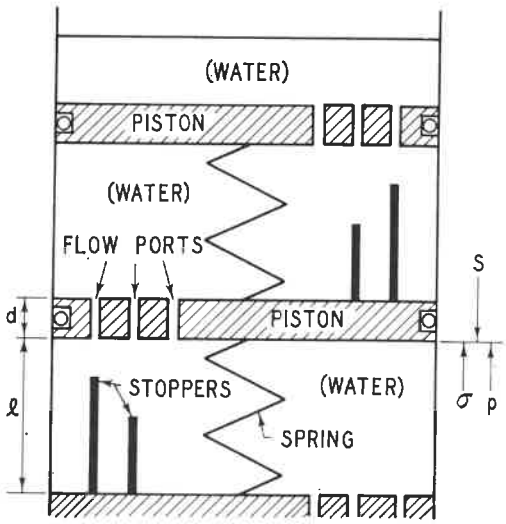

Figure 2. Mechanical model of compaction illustrating that $\sigma = s\text{-}p$ if spring exerts frame pressure, σ. Water flow is so slow that mass accelerations may be ignored.

The porosity will decrease in a systematic way as the frame pressure increases. With reference to the mechanical model of Figure 2, this means that the smaller the porosity $l/(l+d)$ becomes the greater the spring pressure σ will be, because the spring length decreases with the pressure exerted to compress it. Equation (17) states that the porosity will adjust instantaneously to the frame pressure. This assumption is valid only if the frame pressure changes slowly compared with the rate at which the matrix configuration can adjust, as is probably the case. Equation (17) is proposed for compaction, and a different relationship may be required for expansion. By analogy, the springs in Figure 2 need not recover to their original length if the pressure σ is reduced to zero. The mechanical model also will be made more realistic by allowing l to be any arbitrarily decreasing function of σ instead of being linear as required by Hooke's law.

Because the porosity reduction of shales is probably effected by a number of mechanisms, including elastic deformations, breaking of grains, and pressure solution of grains at grain contacts, an empirical correlation rather than a theoretical relation between ϕ and σ is desirable. This could be obtained by plotting values of ϕ vs values of σ obtained for shales in the sedimentary column. According to eq (17) the points plot ed will give a single curve, which is the same for both hyperpressured and normally pressured shales. Hence the curve may be obtained from information on normally pressured shales alone. In particular, if empirical relationships between both ϕ and depth and σ and depth can be obtained for normally pressured shales, a cross plot will give the desired relationship, ϕ vs σ. Athy (1930) gives the empirical relationship

$$\phi_N = \phi_T e^{-b(T-Z)} \tag{18}$$

for shales in north-central Oklahoma which are presumed here to be normally pressured. The porosity for the normally pressured section ϕ_N is a function of the subsurface depth T-Z and constants ϕ_T and b. From eq (18), ϕ_T is the porosity of shale at the surface. The complementary approximate relationship between σ and depth may be obtained by assuming that (a) the water pressure is normal, (b) water and grain compressibilities are negligible, and (c) other rocks in the sedimentary column have about the same density as shale. With these assumptions the normal water pressure p_N is given by

$$p_N = g\rho_w(T-Z)+p_e \tag{19}$$

Substitution of eq (19), (13), and (14) successively into eq (16) gives

$$\begin{aligned}\sigma_N &= S_N - p_N \\ &= S_N - g\rho_w(T-Z) - p_e \\ &= g\int_{Z=Z}^{T} \rho_N dZ - g\rho_w(T-Z) \\ &= g(\rho_r-\rho_w)\int_{Z=Z}^{T}(1-\phi_N)dZ\end{aligned} \tag{20}$$

Substitution of the expression for ϕ_N [eq (18)] into eq (20) and integrating gives

$$\sigma_N = g(\rho_r-\rho_w)\left[(T-Z)-\frac{1}{b}(\phi_T-\phi_T e^{-b(T-Z)})\right] \tag{21}$$

This last equation is the relationship between σ_N and the depth T-Z. Elimination of T-Z between (18) and (21) yields the desired relationship between σ_N and ϕ_N:

$$\sigma_N = \frac{g(\rho_r-\rho_w)}{b}\left[\ln\frac{\phi_T}{\phi_N}-(\phi_T-\phi_N)\right] \tag{22}$$

Because the relationship between σ_N and ϕ_N is the same as the general relationship between σ and ϕ, the subscript N can be eliminated to give the result

$$\sigma = \frac{g(\rho_r-\rho_w)}{b}\left[\ln\frac{\phi_T}{\phi}-(\phi_T-\phi)\right] \tag{23}$$

This equation is presumed to fit an empirical plot of σ vs ϕ for all stages of the compaction of shales. A result of this type could have been obtained using any empirical porosity–depth curve fit.

Because of the empirical nature of eq (23) and the neglect of the compressibilities of water and solid matrix material in deriving it, the introduction of eq (23) into the overall model restricts its validity. This does not seriously impair quantitative conclusions derivable from the model, as the major cause of the increased density and lower porosity of compacting shales is the collapse of the rock frame as a result of the imposed frame pressure σ. This can be demonstrated by deriving the compressibility of the rock frame and making numerical comparisons between this compressibility

and the compressibilities of water and the common mineral constituents of shale.

Differentiation of eq (23) with the neglect of water and mineral compressibilities gives

$$-\frac{d\ln\phi}{d\sigma}=\frac{b}{g(\rho_r-\rho_w)(1-\phi)} \tag{24}$$

The porosity is defined by

$$\phi=(V-V_r)/V \tag{25}$$

where V is the bulk volume and V_r is the volume of solid matrix material contained in V. Differentiation of (25) with V_r constant gives

$$d\ln\phi=\frac{1-\phi}{\phi}d\ln V \tag{26}$$

Substitution of eq (26) back into (24) gives the frame compressibility

$$\begin{aligned}-\frac{d\ln V}{d\sigma}&=\frac{b\phi}{g(\rho_r-\rho_w)(1-\phi)^2} \\ &=1500\times10^{-5}\ \text{atm}^{-1}\ \text{for}\ \phi=\phi_T=0.48 \\ &=270\times10^{-5}\ \text{atm}^{-1}\ \textit{for}\ \phi=0.20 \\ &=110\times10^{-5}\ \text{atm}^{-1}\ \text{for}\ \phi=0.10\end{aligned} \tag{27}$$

The values $b=1.4\times10^{-3}$/m and $\rho_r-\rho_w=1.7$ g/cm^3 used in the computations were taken from Athy (1930). Because σ and the water pressure p usually increase at comparable rates with increasing depth of burial, it is relevant to compare the frame compressibility with the water and mineral compressibilities resulting from the fluid pressure:

$$\begin{aligned}-\frac{d\ln V}{dp}&=-\frac{\partial\ln V}{\partial p}-\frac{\partial\ln V}{\partial t^*}\left(\frac{dt^*}{dp}\right)_{\textit{earth conditions}} \\ &\approx 3\ \text{to}\ 4\times10^{-5}\ \text{atm}^{-1}\end{aligned} \tag{28}$$

for water between 20 and 100°C and 1–500 atm. The symbol t^* is used for temperature.

$$-\frac{d\ln V}{dp}=0.5\text{–}2.8\times10^{-6}\ \text{atm}^{-1} \tag{29}$$

for major mineral constituents of shales. The rock-frame compressibility at 10-percent porosity is greater than the compressibility of water by a factor of about 25–35, and is greater than mineral compressibilities by a larger margin. Thus, porosity and density changes in shales are principally the result of compression of the framework, accompanied by loss of water.

The overall problem is simplified if water and mineral compressibilities are ignored, and an equation for porosity as a function of Z and time can be obtained. In this approximation the continuity equations (8) and (9) become

$$\frac{\partial v_w \phi}{\partial Z} = -\frac{\partial \phi}{\partial t} \tag{30}$$

$$\frac{\partial v_r (1-\phi)}{\partial Z} = \frac{\partial \phi}{\partial t} \tag{31}$$

The coordinate system is fixed at the base of the shale, so v_r is always zero at $Z = 0$, and

$$v^0{}_r = 0 \tag{32}$$

The superscript ^{0} will indicate that a variable is evaluated at $Z = 0$. Because of this condition eq (31) can always be written in the integrated form

$$v_r = \frac{1}{1-\phi} \int_{Z=0}^{Z} \frac{\partial \phi}{\partial t} dZ \tag{33}$$

Equations (30) and (31) may be added together to give

$$\frac{\partial}{\partial Z}\{v_w \phi + v_r (1-\phi)\} = 0 \tag{34}$$

or

$$v_w \phi + v_r (1-\phi) = f(t) \tag{35}$$

a function of time only.

Substituting (33) into (35) and rearranging gives

$$(v_w - v_r)\phi = f(t) - \frac{1}{1-\phi} \int_{Z=0}^{Z} \frac{\partial \phi}{\partial t} dZ \tag{36}$$

The quantity on the LHS of this equation and eq (11) are the same, and may be eliminated to give the result

$$\frac{1}{1-\phi} \int_{Z=0}^{Z} \frac{\partial \phi}{\partial t} dZ = \frac{K}{\mu} \frac{\partial \Psi}{\partial Z} + f(t) \tag{37}$$

The space gradient of the fluid potential $\partial\Psi/\partial Z$ may be expressed in terms of ϕ and derivatives of ϕ as follows:

$$\frac{\partial \psi}{\partial Z} = \frac{\partial p}{\partial Z} + g\rho_w \qquad \text{[eq (12)]} \tag{38}$$

$$= \frac{\partial S}{\partial Z} - \frac{\partial \sigma}{\partial Z} + g\rho_w \qquad \text{[eq (16)]} \tag{39}$$

$$= \frac{g(\rho_r - \rho_w)(1-\phi)}{b\phi}\left(\frac{\partial \phi}{\partial Z} - b\phi\right) \qquad \text{[eqs (15) and (23)]} \tag{40}$$

The last result may be substituted into eq (37) to give

$$\frac{1}{1-\phi} \int_{Z=0}^{Z} \frac{\partial \phi}{\partial t} dZ = \frac{Kg(\rho_r - \rho_w)(1-\phi)}{\mu b \phi}\left(\frac{\partial \phi}{\partial Z} - b\phi\right) + f(t) \tag{41}$$

At $Z = 0$ the integral on the LHS is zero so that $f(t)$ may be eliminated:

$$\frac{1}{1-\phi}\int_{Z=0}^{Z}\frac{\partial\phi}{\partial t}\,dZ = \frac{Kg(\rho_r-\rho_w)(1-\phi)}{\mu b\phi}\left(\frac{\partial\phi}{\partial Z}-b\phi\right)- \frac{K^0 g(\rho_r-\rho_w)(1-\phi^0)}{\mu^0 b\phi^0}\left(\frac{\partial\phi^0}{\partial Z}-b\phi^0\right) \tag{42}$$

It is expected that the permeability constant K will be a sensitive function of porosity for a given shale-rock type. The following formula has been used in numerical calculations, as it embraces both the theoretical Kozeny relation and the empirical relationships found by Vasquez for very fine sand and chalk (Pirson, 1963, p. 5):

$$K = h\phi^a/(1-\phi)^c \tag{43}$$

The constants h, a, and c must be established empirically. Archie (Pirson, 1963, p. 5) has shown that a number of sand-rock types have permeabilities which increase exponentially with the porosity, and this type of dependence may be incorporated in future numerical work. However, few permeability measurements are currently available for shales and the actual dependence on porosity remains to be determined. The mechanical model of Figure 2 shows how the permeability can be made to depend strongly on porosity.

When eq (43) is substituted into eq (42), the resulting equation gives the porosity at each point Z throughout a shale unit as a function of time, of Z, and of the history of the unit. In obtaining solutions to the equation, the dependence of the viscosity on temperature and pressure and salinity have been taken from the literature.

BOUNDARY CONDITIONS

The simplest boundary condition at the base of the shale unit is that the permeability of the underlying substratum is zero. For this condition eq (42) simplifies to

$$\frac{1}{1-\phi}\int_{Z=0}^{Z}\frac{\partial\phi}{\partial t}\,dZ = \frac{Kg(\rho_r-\rho_w)(1-\phi)}{\mu b\phi}\left(\frac{\partial\phi}{\partial Z}-b\phi\right) \tag{44}$$

This problem will be referred to as case 1 for brevity.

A second interesting boundary condition for $Z = 0$, to be referred to as case 2, is that the underlying unit is normally pressured. For this condition eq (42) is unaltered, but a second equation is obtained for simultaneous solution with eq (42). The necessary result is obtained by writing down and equating two expressions for the frame pressure at $Z = 0$:

$$\sigma^0 = \frac{g(\rho_r-\rho_w)}{b}\left[\ln\frac{\phi_T}{\phi^0}-(\phi_T-\phi^0)\right] \quad \text{[eq (23)]} \tag{45}$$

$$= S^0 - p^0{}_N \quad \text{[eq (16)]} \tag{46}$$

$$= g(\rho_r-\rho_w)\int_{Z=0}^{T}(1-\phi)\,dZ \quad \text{[eqs (15) and (19)]} \tag{47}$$

Elimination of common factors from (45) and (47) gives the required result:

$$\ln\frac{\phi_T}{\phi^0}-(\phi_T-\phi^0)=b\int_{Z=0}^{T}(1-\phi)\,dZ \tag{48}$$

Equations (47) and (48) are valid during shale deposition and during any time lapse after shale deposition but before deposition of any succeeding unit. When a succeeding unit is being or has been added over the shale, these two equations require an additional term. If the thickness of the overlying unit is D (Figure 1) and the bulk density of the water-saturated rock is ρ_s, then

$$S^0-p^0{}_N=g(\rho_r-\rho_w)\int_{Z=0}^{T_s}(1-\phi)\,dZ+g(\rho_s-\rho_w)D \tag{49}$$

where T_s is the Z coordinate of the top of the shale unit, and

$$\ln\frac{\phi_T}{\phi^0}-(\phi_T-\phi^0)=b\int_{Z=0}^{T_s}(1-\phi)dZ+b\left(\frac{\rho_s-\rho_w}{\rho_r-\rho_w}\right)D \tag{50}$$

It is assumed that ρ_s is independent of time and is constant for the overlying unit.

All the following conditions apply to both case 1 and case 2.

The porosity at the top of the shale unit during deposition or before the addition of overlying sediments must be ϕ_T, according to eq (23), because the frame pressure will be zero. If a thickness D of normally pressured sediments has been added to the top of the unit the porosity at the top ϕ^* is computed from

$$ln\frac{\phi_T}{\phi^*}-(\phi_T-\phi^*)=b\left(\frac{\rho_s-\rho_w}{\rho_r-\rho_w}\right)D \tag{51}$$

During the deposition of the shale, the condition that has been adopted in computations is that the thickness T of the shale increases linearly with time t:

$$\begin{aligned} T&=et\\ e&=\text{const}\end{aligned} \tag{52}$$

After cessation of shale deposition the shale unit thickness T_s will tend to decrease as water is lost, whether other sediments are being added or not. During all these succeeding epochs there is a further condition that the mass of the solid framework (grains) M per unit area of the shale does not change:

$$M=\rho_r\int_{Z=0}^{T_s}(1-\phi)dZ=\text{const} \tag{53}$$

This relationship provides a simultaneous condition on T_s and the porosity profile through the shale.

NUMERICAL SOLUTIONS

Solutions to the problem of shale compaction have been obtained for case 1 (under-

lying unit impermeable) and case 2 (underlying unit normally pressured). For both cases the sequence of processes were as follows.

1. The deposition of 320 m of shale at a rate of 0.1 m/1000 yr, requiring 3.2×10^6 yr.
2. The passage of 10^5 yr during which no further deposition occurs.
3. The deposition of 600 m of normally pressured sediments over the shale at a rate of 0.5 m/1000 yr, requiring 1.2×10^6 yr.
4. The passage of 2.0×10^6 yr during which no further deposition occurs.

In carrying out the computations it was assumed that the permeability of the shales varies as the eighth power of the porosity, as Vasquez (Pirson, 1963) found for fine sands, so that $a = 8$ and $c = 0$ in eq (43). The constant h was determined by requiring that $K = 10^{-5}$ md for $\phi = 0.20$. Shale permeabilities of this order of magnitude have been reported by Gondouin and Scala (1958) The grain density of the shale ρ_r was assumed to be 2.65 g/cc, and the bulk density of the overlying sediments ρ_s was taken to be 2.2 g/cc. The constants of eq (18) were $\phi_T = 0.48$ and $b = 0.0014$/m, as determined by Athy (1930) for north-central Oklahoma and neighboring areas of Kansas; different constants or even a different equation would be needed for other areas. The dependence of the viscosity of water on temperature and salinity was obtained from the compilation of Fabuss and Korosi (1968). The pore water was assumed to contain 5 percent sodium chloride. Temperature as a function of depth was computed assuming 10°C for the sediment–water interface and a geothermal gradient of 0.03°C/m.

The results of the computations are shown in Tables 1, 2, 3, and 4 for case 1 and Tables 5, 6, 7, and 8 for case 2. The depth from the top of the shale is given in the right-hand column. The other columns, from left to right, give the following

1. Fractional porosity of the shale.
2. Normal porosity of the shale, which is the value which would be approached after a long time lapse without further deposition, during which time the pore pressure would also approach normal.
3. The pore-water pressure minus the fluid pressure at the top of the shale formation in bars (1 bar = 0.987 atm = 14.5 psi).
4. The excess water pressure, in bars. This is the pore-water pressure minus the normal hydrostatic pressure for the subsurface depth in question.
5. The overburden pressure or total vertical stress in bars, minus the pressure of the overlying water and atmosphere. This is the total weight, per cm^2, of water-saturated rock overlying the depth in question.
6. The frame pressure in bars. This is the difference between overburden pressure and pore-water pressure, and is the force per unit area acting to collapse the rock framework and reduce the porosity. This pressure is responsible for the slow expulsion of water from the low-permeability shale.
7. Permeability, in microdarcies, μd.
8. Velocity of water being squeezed out of the compacting shale, relative to the

Table 1. Shale Properties Immediately After Deposition—Impermeable Substratum

Fractional porosity (1)	Normal porosity (2)	Pore-water pressure, bars (3)	Excess-water pressure, bars (4)	Over-burden pressure, bars (5)	Frame pressure, bars (6)	Permeability, μd (7)	Water velocity through rock, cm/10^3 yr (8)	Water flow rate, cm^3 water/ cm^2 rock/ 10^3 yr (9)	Rock velocity, cm/10^3 yr (10)	Depth of burial, m (11)
0.4800	0.4800	0.0	0.0	0.0	0.0	11.01	13.5	6.47	−6.47	0.0
0.4672	0.4667	2.1	0.05	3.7	1.62	8.86	12.5	5.83	−5.83	20.0
0.4547	0.4539	4.2	0.12	7.4	3.26	7.14	11.5	5.23	−5.23	40.0
0.4426	0.4413	6.3	0.18	11.2	4.95	5.76	10.5	4.67	−4.67	60.0
0.4309	0.4291	8.4	0.26	15.0	6.66	4.65	9.63	4.15	−4.15	80.0
0.4195	0.4173	10.5	0.33	18.9	8.41	3.75	8.74	3.67	−3.67	100.0
0.4085	0.4058	12.6	0.42	22.8	10.18	3.03	7.87	3.21	−3.21	120.0
0.3977	0.3946	14.7	0.51	26.7	11.99	2.44	7.02	2.79	−2.79	140.0
0.3873	0.3837	16.8	0.60	30.6	13.82	1.98	6.20	2.40	−2.40	160.0
0.3771	0.3731	18.9	0.70	34.6	15.69	1.60	5.39	2.03	−2.03	180.0
0.3672	0.3628	21.1	0.80	38.6	17.57	1.29	4.59	1.69	−1.69	200.0
0.3575	0.3528	23.2	0.90	42.7	19.50	1.04	3.81	1.36	−1.36	220.0
0.3482	0.3430	25.3	1.00	46.7	21.45	0.84	3.03	1.06	−1.06	240.0
0.3389	0.3335	27.4	1.09	50.9	23.45	0.68	2.27	0.77	−0.77	260.0
0.3299	0.3243	29.5	1.17	55.0	25.48	0.55	1.51	0.50	−0.50	280.0
0.3210	0.3154	31.6	1.22	59.2	27.57	0.44	0.75	0.24	−0.24	300.0
0.3123	0.3067	33.6	1.25	63.4	29.71	0.35	0.0	0.0	0.0	320.0

Table 2. Shale Properties Following Deposition and Time Lapse of 10^5 yr—Impermeable Substratum

Fractional porosity (1)	Normal porosity (2)	Pore-water pressure, bars (3)	Excess-water pressure, bars (4)	Over-burden pressure, bars (5)	Frame pressure, bars (6)	Permeability, μd (7)	Water velocity through rock, cm/10^3 yr (8)	Water flow rate, cm^3 water/ cm^2 rock/ 10^3 yr (9)	Rock velocity, cm/10^3 yr (10)	Depth of burial, m (11)
0.4800	0.4800	0.0	0.0	0.0	0.0	11.0	0.84	0.40	−0.40	0.0
0.4676	0.4677	1.9	0.0	3.4	1.6	8.93	0.86	0.40	−0.40	18.6
0.4548	0.4547	3.9	0.01	7.2	3.3	7.15	0.87	0.40	−0.40	38.6
0.4422	0.4422	5.9	0.01	11.0	5.0	5.71	0.88	0.39	−0.39	58.6
0.4301	0.4300	8.0	0.02	14.8	6.8	4.58	0.89	0.38	−0.38	78.6
0.4182	0.4181	10.0	0.02	18.6	8.6	3.66	0.88	0.37	−0.37	98.6
0.4068	0.4066	12.1	0.04	22.5	10.5	2.93	0.87	0.35	−0.35	118.6
0.3956	0.3953	14.1	0.04	26.4	12.4	2.34	0.84	0.33	−0.33	138.6
0.3848	0.3844	16.1	0.06	30.4	14.3	1.88	0.80	0.31	−0.31	158.6
0.3742	0.3738	18.1	0.06	34.4	16.2	1.50	0.76	0.28	−0.28	178.6
0.3640	0.3635	20.2	0.10	38.4	18.2	1.20	0.69	0.25	−0.25	198.6
0.3539	0.3534	22.2	0.10	42.5	20.2	0.96	0.61	0.22	−0.22	218.6
0.3443	0.3437	24.3	0.13	46.6	22.3	0.77	0.52	0.18	−0.18	238.6
0.3348	0.3342	26.3	0.13	50.7	24.4	0.62	0.41	0.14	−0.14	258.6
0.3257	0.3250	28.4	0.17	54.8	26.5	0.50	0.28	0.091	−0.091	278.6
0.3167	0.3160	30.4	0.15	59.0	28.6	0.40	0.14	0.046	−0.046	298.6
0.3081	0.3073	32.4	0.18	63.2	30.8	0.32	0.0	0.0	−0.0	318.6

Table 3. Shale Properties After Deposition of 600 m of Overlying Sediments—Impermeable Substratum

Fractional porosity (1)	Normal porosity (2)	Pore-water pressure, bars (3)	Excess-water pressure, bars (4)	Over-burden pressure, bars (5)	Frame pressure, bars (6)	Permeability, $\mu d \times 10^2$ (7)	Water velocity through rock, cm/10^3 yr (8)	Water flow rate, cm^3 water/cm^2 rock/10^3 yr (9)	Rock velocity, cm/10^3 yr (10)	Depth, m (11)
0.1973	0.1973	60.7	0.0	129.5	68.7	0.90	9.99	1.97	−1.97	0.0
0.2045	0.1950	65.9	4.32	131.4	65.5	1.20	9.08	1.86	−1.86	8.5
0.2139	0.1896	74.5	10.85	135.9	61.5	1.71	7.56	1.62	−1.62	28.5
0.2186	0.1844	80.9	15.27	140.4	59.5	2.04	6.46	1.41	−1.41	48.5
0.2211	0.1793	86.4	18.75	144.9	58.5	2.23	5.56	1.23	−1.23	68.5
0.2217	0.1743	91.2	21.47	149.4	58.3	2.28	4.79	1.06	−1.06	88.5
0.2216	0.1695	95.6	23.91	153.9	58.3	2.28	4.08	0.91	−0.91	108.5
0.2203	0.1648	99.6	25.83	158.4	58.9	2.16	3.43	0.76	−0.76	128.5
0.2187	0.1603	103.5	27.69	162.9	59.5	2.05	2.81	0.62	−0.62	148.5
0.2159	0.1558	106.8	29.04	167.4	60.6	1.85	2.23	0.48	−0.48	168.5
0.2133	0.1515	110.3	30.44	171.9	61.7	1.68	1.65	0.35	−0.35	188.5
0.2093	0.1474	113.1	31.23	176.5	63.4	1.44	1.10	0.23	−0.23	208.5
0.2055	0.1433	116.0	32.10	181.0	65.1	1.24	5.48	0.11	−0.11	228.5
0.1999	0.1393	118.0	32.13	185.6	67.5	1.00	0.0	0.0	0.0	248.5

Table 4. Shale Properties 2×10^6 yr After Burial Beneath 600 m of Sediments—Impermeable Substratum

Fractional porosity (1)	Normal porosity (2)	Pore-water pressure, bars (3)	Excess-water pressure, bars (4)	Over-burden pressure, bars (5)	Frame pressure, bars (6)	Permeability, μd $\times 10^3$ (7)	Water velocity through rock, cm/10^3 yr (8)	Water flow rate, cm^3 water/ cm^2 rock/ 10^3 yr (9)	Rock velocity, cm/10^3 yr (10)	Depth, m (11)
0.1973	0.1973	60.7	0.0	129.5	68.7	8.97	0.91	0.18	−0.18	0.0
0.1948	0.1923	63.8	1.2	133.7	69.9	8.09	0.91	0.18	−0.18	18.4
0.1920	0.1870	67.1	2.4	138.3	71.2	7.22	0.89	0.17	−0.17	38.4
0.1897	0.1818	70.5	3.9	142.8	72.3	6.55	0.86	0.16	−0.16	58.4
0.1872	0.1768	73.9	5.2	147.4	73.5	5.89	0.80	0.15	−0.15	78.4
0.1850	0.1719	77.4	6.7	152.1	74.6	5.36	0.73	0.14	−0.14	98.4
0.1824	0.1672	80.7	8.0	156.7	75.9	4.79	0.65	0.12	−0.12	118.4
0.1801	0.1625	84.2	9.4	161.3	77.1	4.33	0.56	0.10	−0.10	138.4
0.1772	0.1580	87.3	10.5	165.9	78.6	3.79	0.46	0.081	−0.081	158.4
0.1745	0.1537	90.5	11.7	170.6	80.1	3.36	0.35	0.061	−0.061	178.4
0.1709	0.1494	93.2	12.4	175.2	82.0	2.85	0.24	0.041	−0.041	198.4
0.1676	0.1453	96.0	13.2	179.9	83.8	2.43	0.12	0.020	−0.020	218.4
0.1631	0.1413	98.1	13.2	184.5	86.4	1.95	0.0	0.0	0.0	238.4

Table 5. Shale Properties Immediately After Deposition—Normally Pressured Substratum

Fractional porosity (1)	Normal porosity (2)	Pore-water pressure, bars (3)	Excess-water pressure, bars (4)	Over-burden pressure, bars (5)	Frame pressure, bars (6)	Permeability, μd (7)	Water velocity through rock, cm/10^3 yr (8)	Water flow rate, cm^3 water/ cm^2 rock/ 10^3 yr (9)	Rock velocity, cm/10^3 yr (10)	Depth of burial, m (11)
0.4800	0.4800	0.0	0.0	0.0	0.0	11.0	1.57	0.75	−6.62	0.0
0.4671	0.4667	2.1	0.05	3.7	1.6	8.85	1.41	0.66	−5.97	20.0
0.4546	0.4539	4.1	0.09	7.4	3.2	7.12	1.25	0.57	−5.36	40.0
0.4424	0.4413	6.2	0.14	11.2	5.0	5.73	1.11	0.49	−4.80	60.0
0.4305	0.4291	8.3	0.20	15.0	6.7	4.61	0.96	0.42	−4.27	80.0
0.4190	0.4173	10.4	0.25	18.9	8.5	3.71	0.83	0.35	−3.78	100.0
0.4078	0.4058	12.5	0.31	22.8	10.3	2.99	0.69	0.28	−3.32	120.0
0.3968	0.3946	14.5	0.36	26.7	12.1	2.40	0.56	0.22	−2.89	140.0
0.3861	0.3837	16.6	0.41	30.6	14.0	1.93	0.43	0.17	−2.49	160.0
0.3757	0.3731	18.7	0.46	34.6	15.9	1.55	0.30	0.11	−2.11	180.0
0.3655	0.3628	20.7	0.49	38.6	17.9	1.25	0.17	0.06	−1.76	200.0
0.3555	0.3528	22.8	0.51	42.7	19.9	1.00	0.04	0.01	−1.43	220.0
0.3457	0.3430	24.8	0.51	46.8	22.0	0.80	−0.09	−0.03	−1.11	240.0
0.3360	0.3335	26.8	0.47	50.9	24.1	0.63	−0.21	−0.07	−0.81	260.0
0.3263	0.3243	28.7	0.39	55.0	26.3	0.50	−0.34	−0.11	−0.53	280.0
0.3167	0.3154	30.6	0.24	59.2	28.6	0.40	−0.48	−0.15	−0.26	300.0
0.3070	0.3067	32.4	0.00	63.4	31.0	0.31	−0.59	−0.18	0.0	320.0

Table 6. Shale Properties Following Deposition and Time Lapse of 10^5 yr—Normally Pressured Substratum

Fractional porosity (1)	Normal porosity (2)	Pore-water pressure, bars (3)	Excess-water pressure, bars (4)	Over-burden pressure, bars (5)	Frame pressure, bars (6)	Permeability, μd (7)	Water velocity through rock, cm/10^3 yr $\times 10^3$ (8)	Water flow rate, cm^3 water/cm^2 rock/10^3 yr $\times 10^3$ (9)	Rock velocity, cm/10^3 yr $\times 10^3$ (10)	Depth of burial, m (11)
0.4800	0.4800	0.0	0.0	0.0	0.0	11.0	22.2	10.7	−54.3	0.0
0.4673	0.4673	1.9	0.00	3.5	1.6	8.88	11.7	5.45	−54.1	19.2
0.4544	0.4544	4.0	0.00	7.3	3.3	7.10	6.12	2.78	−53.3	39.2
0.4419	0.4418	6.0	0.00	11.1	5.1	5.68	6.67	2.95	−51.8	59.2
0.4297	0.4296	8.0	0.00	14.9	6.9	4.54	7.01	3.01	−49.8	79.2
0.4178	0.4178	10.0	0.00	18.7	8.7	3.63	7.02	2.93	−47.0	99.2
0.4063	0.4062	12.1	0.00	22.6	10.5	2.90	6.67	2.71	−43.7	119.2
0.3951	0.3950	14.1	0.00	26.5	12.5	2.32	5.95	2.35	−39.7	139.2
0.3841	0.3841	16.1	0.00	30.5	14.4	1.85	4.88	1.88	−35.0	159.2
0.3735	0.3735	18.1	0.01	34.5	16.4	1.48	3.47	1.30	−29.9	179.2
0.3632	0.3632	20.2	0.01	38.5	18.4	1.18	1.77	0.64	−24.4	199.2
0.3532	0.3532	22.2	0.01	42.6	20.4	0.95	−0.16	−0.06	−18.7	219.3
0.3435	0.3434	24.2	0·01	46.7	22.5	0.76	−2.19	−0.75	−13.1	239.2
0.3340	0.3339	26.2	0.01	50.8	24.6	0.60	−4.16	−1.39	−8.04	259.2
0.3247	0.3247	28.3	0.00	55.0	26.7	0.48	−5.90	−1.92	−3.85	279.2
0.3158	0.3157	30.3	0.00	59.1	28.9	0.39	−7.09	−2.24	−1.02	299.2
0.3070	0.3070	32.3	0.00	63.3	31.0	0.31	−5.99	−1.84	0.0	319.2

Table 7. Shale Properties After Deposition of 600 m of Overlying Sediments—Normally Pressured Substratum

Fractional porosity (1)	Normal porosity (2)	Pore-water pressure, bars (3)	Excess-water pressure, bars (4)	Over-burden pressure, bars (5)	Frame pressure, bars (6)	Permeability, $\mu d \times 10^2$ (7)	Water velocity through rock, cm/10^3 yr (8)	Water flow rate, cm^3 water/cm^2 rock/10^3 yr (9)	Rock velocity, cm/10^3 yr (10)	Depth, m (11)
0.1973	0.1973	60.7	0.0	129.5	68.7	0.90	1.08	0.21	−2.06	0.0
0.2048	0.1938	67.0	4.97	132.3	65.4	1.21	0.93	0.19	−1.89	12.6
0.2100	0.1895	72.9	9.26	136.0	63.1	1.48	0.782	0.16	−1.70	28.6
0.2134	0.1833	79.8	13.69	141.4	61.6	1.68	0.602	0.13	−1.45	52.6
0.2138	0.1772	85.3	16.84	146.8	61.5	1.71	0.455	0.10	−1.23	76.6
0.2122	0.1714	90.1	19.18	152.2	62.1	1.61	0.323	0.07	−1.03	100.6
0.2091	0.1657	94.2	20.85	157.7	63.5	1.43	0.199	0.04	−0.84	124.6
0.2044	0.1602	97.6	21.85	163.1	65.5	1.19	0.080	0.02	−0.66	148.6
0.1954	0.1532	100.8	21.83	170.4	69.6	0.83	−0.078	−0.02	−0.44	180.6
0.1892	0.1498	101.5	20.90	174.1	72.6	0.64	−0.160	−0.03	−0.33	196.6
0.1808	0.1465	101.1	18.80	177.8	76.7	0.45	−0.245	−0.04	−0.23	212.6
0.1682	0.1433	98.0	14.12	181.5	83.5	0.25	−0.339	−0.06	−0.12	228.6
0.1602	0.1417	95.2	10.55	183.4	88.1	0.17	−0.494	−0.08	−0.06	236.6
0.1420	0.1401	85.5	0.00	185.3	99.8	0.06	−0.471	−0.07	0.0	244.6

Table 8. Shale Properties 2×10^6 yr After Burial Beneath 600 m of Sediments—Normally Pressured Substratum

Fractional porosity (1)	Normal porosity (2)	Pore-water pressure, bars (3)	Excess-water pressure, bars (4)	Over-burden pressure, bars (5)	Frame pressure, bars (6)	Permeability, μd $\times 10^3$ (7)	Water velocity through rock, cm/10^3 yr $\times 10^2$ (8)	Water flow rate, cm^3 water/ cm^2 rock/ 10^3 yr $\times 10^2$ (9)	Rock velocity, cm/10^3 yr $\times 10^2$ (10)	Depth, m (11)
0.1973	0.1973	60.7	0.0	129.5	68.7	8.97	4.74	0.94	−9.72	0.0
0.1937	0.1929	62.8	0.38	133.2	70.4	7.73	4.70	0.91	−9.64	16.3
0.1894	0.1875	65.3	0.89	137.8	72.5	6.46	4.54	0.86	−9.33	36.3
0.1853	0.1824	67.9	1.46	142.4	74.5	5.42	4.23	0.78	−8.79	56.3
0·1813	0.1773	70.5	2.05	147.0	76.5	4.56	3.73	0.68	−8.03	76.3
0.1774	0.1724	73.1	2.63	151.6	78.5	3.83	3.05	0.54	−7.08	96.3
0.1735	0.1677	75.7	3.15	156.3	80.6	3.21	2.22	0.39	−5.97	116.3
0·1694	0.1630	78.1	3.56	160.9	82.8	2.65	1.26	0.21	−4.75	136.3
0.1651	0.1585	80.3	3.76	165.6	85.3	2.16	0.22	0.04	−3.49	156.3
0.1604	0.1542	82.2	3.67	170.3	88.0	1.71	−0.09	−0.14	−2.26	176.3
0.1551	0.1499	83.8	3.15	175.0	91.2	1.31	−1.99	−0.29	−1.17	196.3
0.1490	0.1458	84.6	2.00	179.7	95.0	0.95	−2.72	−0.41	−0.034	216.3
0.1420	0.1417	84.6	0.00	184.4	99.8	0.64	−3.11	−0.44	−0.0	236.3

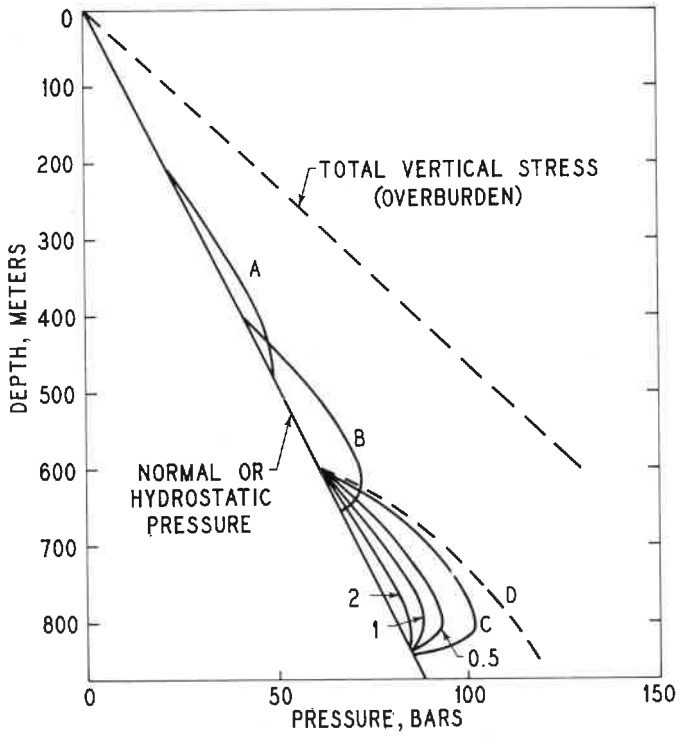

Figure 3. Pressure history for shale unit with underlying and overlying normally pressured sands after burial to depths of 200 m (A), 400 m (B), and 600 m (C). Pressures following burial to 600 m and further time lapses of 0.5, 1.0, and 2.0 $\times 10^6$ yr are shown. Curve D differs from curve C only in that shale has an impermeable base.

matrix material, in cm/1000 yr. After cessation of sedimentation, this flow will gradually decrease to zero as the shale becomes normally pressured.

9. Volume flow rate of water relative to the rock matrix, in cm^3 water/cm^2 rock/1000 yr.

10. Velocity of the compacting rock matrix relative to the base of the shale unit, in cm/1000 yr.

The examples discussed here, and other examples which have been worked, show that a portion of the shale next to a normally pressured sand tends to become compressed as the overburden is increased and the permeability is greatly reduced. This is most evident in Table 3. The effect is reflected in Figure 3, which gives a detailed pressure history for case 2. The high fluid pressure developed in this example is effectively dissipated in about 2×10^6 yr. However, if either calculation is repeated, changing the initial shale thickness to 1000 m and the depth of burial to 1300 m, high

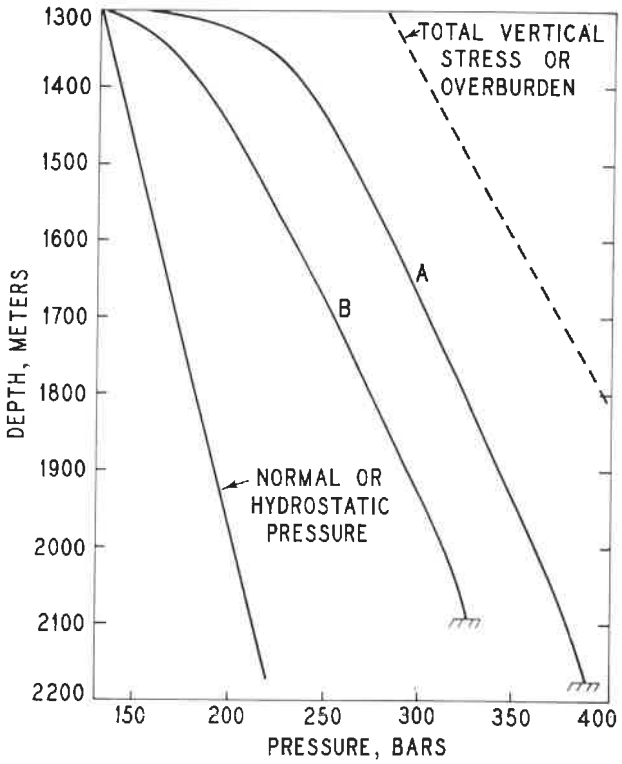

Figure 4. Curve A gives pore-water pressure within shale immediately after deposition of 1300 m of sediments over shale. Curve B gives pore-water pressure after 10^8 yr.

pressures are developed and persist for more than 10^8 yr (Fig. 4). It may be concluded that the effect under investigation is a major contributor to high pressures in the earth.

The solutions to the equations describing shale compaction were obtained using a digital computer and a finite difference technique.

DISCUSSION

The present model of shale compaction is considered suitable for treating the sedimentation and compaction of several layers of sand and shale simultaneously, as long as the flow of water is vertical. In situations where considerable horizontal flow within shales is expected, the compaction problem will require treatment in three space dimensions, and additional mechanical properties of shales and surrounding rocks must be known to take into account lateral expansion or contraction of the rock framework.

The model can be generalized to take into account what seems to be an overall decrease in porosity over hundreds of millions of years in normally pressured shales,

which is a time effect. This porosity decrease might accompany very slow chemical changes such as the alteration of montmorillonite to illite (Weaver, 1967). This factor can be taken into account by letting the constants ϕ_T and b of eq (18) be functions of time.

Elliott (1970) has questioned the empirical exponential dependence of normal porosity on depth of burial given by Athy (1930) and used in the present development. He has found that Athy's relation, combined with the likely assumption that shale interval travel time is a linear function of porosity, yields a shale velocity vs depth curve which is concave toward the velocity axis. Experience shows that the shale velocity vs depth curve should be convex toward the velocity axis, as summarized by the empirical relationship (Faust, 1951; Pennebaker, 1968)

$$v = \alpha(T-Z)^{\frac{1}{n}}$$

where v is the sonic velocity, α and n are constants, and $T-Z$ is the depth.

ACKNOWLEDGMENTS

The author acknowledges the suggestions of his colleagues and specifically the help of G. C. Dysinger with computational techniques and R. S. Scalan who helped check the programs.

REFERENCES

Athy, L. F., 1930, Density, porosity, and compaction of sedimentary rocks: Am. Assoc. Petroleum Geologists Bull., v. 14, no. 1, p. 1–22.

Boatman, W. A., Jr., 1967, Measuring and using shale density to aid in drilling wells in high-pressure areas: Jour. Petrol. Tech., v. 19, no. 5, p. 1423–1429.

Burst, J. F., 1969, Diagenesis of Gulf Coast clayey sediments and its possible relation to petroleum migration: Am. Assoc. Petroleum Geologists Bull., v. 53, no. 1, p. 73–93.

Chaney, P. E., 1950, Abnormal pressures and lost circulation: World Oil, v. 130, no. 5, p. 122–126.

Dickinson, G., 1953, Geological aspects of abnormal reservoir pressures in Gulf Coast Louisiana: Am. Assoc. Petroleum Geologists Bull., v. 25, no. 10, p. 410–432.

Elliott, S. E., 1970, personal communication.

Fabuss, B. M., and Korosi, A., 1968, Properties of sea water and solutions containing sodium chloride, potassium chloride, sodium sulfate and magnesium sulfate: Office of Saline Water R & D Progress Report No. 384, 143 p.

Faust, L. Y., 1951, Seismic velocity as a function of depth and geologic time: Geophysics, v. 16, no. 1, p. 192–206.

Finch, W. C., 1969, Abnormal pressure in the Antelope field, North Dakota: Jour. Pet. Tech., v. 21, no. 7, p. 821–826.

Gondouin, M., and Scala, C., 1958, Streaming potential and the SP log: Petrol. Trans. AIME, v. 213, p. 170–179.

Hanshaw, B. B., 1962, Membrane properties of compacted clays: unpubl. doctor's dissertation, Harvard Univ., 132 p.

Harkins, K. L., and Baugher, J. W., III, 1969, Geological significance of abnormal formation pressures: Jour. Petrol. Tech., v. 21, no. 8, p. 961–966.

Heard, H. C., and Rubey, W. W., 1966, Tectonic implications of gypsum dehydration: Geol. Soc. America Bull., v. 77, no. 7, p. 741–760.

Pennebaker, E. S., 1968, An engineering interpretation of seismic data: paper no. 2165 presented at 43rd annual meeting of SPE of AIME (Houston, Texas).

Pirson, S. J., 1963, Handbook of well log analysis: Prentice-Hall, Inc., Englewood Cliffs, New Jersey, 326 p.

Powers, M. C., 1967, Fluid-release mechanisms in compacting marine mudrocks and their importance in oil exploration: Am. Assoc. Petroleum Geologists Bull., v. 53, no. 1, p. 1240–1254.

Rubey, W. W., and Hubbert, M. K., 1959, Role of fluid pressure in mechanics of overthrust faulting: Am. Assoc. Petroleum Geologists Bull., v. 70, no. 2, p. 167–184.

Tkhostov, B. A., 1963, Initial rock pressures in oil and gas deposits: The Macmillan Co., New York, 118 p.

Weaver, C. E., 1967, Potassium, illite, and the ocean: Geochem. et Cosmochem. Acta, v. 31, p. 2181–2196.